Journal of Applied Physics

Thermal properties, magneto- and barocaloric effects in $La_{0.7}Pb_{0.3}MnO_3$ single crystal

Cite as: J. Appl. Phys. **113**, 073901 (2013); https://doi.org/10.1063/1.4792044
Submitted: 23 October 2012 . Accepted: 29 January 2013 . Published Online: 15 February 2013

A. V. Kartashev, E. A. Mikhaleva, M. V. Gorev, E. V. Bogdanov, A. V. Cherepakhin, K. A. Sablina, N. V. Mikhashonok, I. N. Flerov, and N. V. Volkov

Thermal properties, magneto- and baro-caloric effects in $La_{0.7}Pb_{0.3}MnO_3$ single crystal

A. V. Kartashev,[1,2,a)] E. A. Mikhaleva,[1,2] M. V. Gorev,[1,2] E. V. Bogdanov,[1] A. V. Cherepakhin,[1] K. A. Sablina,[1] N. V. Mikhashonok,[1] I. N. Flerov,[1,2] and N. V. Volkov[1,2]
[1]*Kirensky Institute of Physics SB RAS, Krasnoyarsk 660036, Russia*
[2]*Siberian Federal University, Krasnoyarsk 660079, Russia*

(Received 23 October 2012; accepted 29 January 2013; published online 15 February 2013)

The results of heat capacity, thermal dilatation and T-p phase diagram studies on the $La_{0.7}Pb_{0.3}MnO_3$ single crystal are reported. Direct measurements of intensive magnetocaloric effect are performed by means of adiabatic calorimeter. Barocaloric effect is determined using data of heat capacity and susceptibility to hydrostatic pressure. Caloric efficiency of manganite in the vicinity of ferromagnetic phase transition is discussed and compared with that of other magnetic materials. © *2013 American Institute of Physics*. [http://dx.doi.org/10.1063/1.4792044]

I. INTRODUCTION

Among magnetic substances, the family of manganites is one of the most popular for investigations in the field of phase transitions, multiferroicity, magnetocaloric effect (MCE), and other interesting and important physical phenomena. Very often these compounds are based on $LaMnO_3$ with the substitution of La^{3+} ion by divalent and/or trivalent cations. Many crystals of such a general composition $(La^{3+}{}_{1-y}Me^{3+}{}_y)_{1-x}Me^{2+}{}_x\ Mn^{3+}{}_{1-x}Mn^{4+}{}_x\ O_3$ undergoing ferro- and antiferro-magnetic phase transitions have been investigated, mainly in relation to their magnetic and transport properties. However, thermal properties of manganites have been studied less intensively. For example, we are unaware of any data concerning thermal dilatation and temperature-pressure phase diagrams. However, many papers are devoted to studies of MCE.[1–6] As a rule, instead of direct measurements, the values of both extensive ΔS_{MCE} and intensive $\Delta T^{MCE}{}_{AD}$ MCE have been determined from the analysis of the magnetisation temperature dependence M(T) in accordance with the expressions,[1]

$$\Delta S_{MCE} = \int_0^H \left(\frac{\partial M}{\partial T}\right)_{p,H} dH, \tag{1}$$

$$\Delta T_{AD}^{MCE} = -\frac{T}{C_{p,H}} \int_0^H \left(\frac{\partial M}{\partial T}\right)_{p,H} dH. \tag{2}$$

Rarely, MCE has been determined by considering the temperature dependencies of the heat capacity at different magnetic fields H, as was done for $(La_{0.55}Bi_{0.15})Ca_{0.3}MnO_3$ in Ref. 7. They analysed the behaviour of total entropy S(T,H) consisting of the lattice contribution S_{LAT} (T) and the anomalous part ΔS(T,H) associated with the order parameter (magnetisation M). In this case, the extensive MCE was evaluated as the entropy change with magnetic field variation $\Delta S_{MCE} = S_{H\neq 0} - S_{H=0}$ at constant temperature.

Direct measurements of intensive MCE have seldom been carried out[8,9] and the investigators did not try to maintain real adiabatic conditions, supposing that it was enough to perform a rather quick process of magnetic field change. On the other hand, it is known that the most correct and reliable way to determine the real values of intensive caloric effects of different physical nature is to perform direct measurements of ΔT_{AD} by means of an adiabatic calorimeter. Recently, we have succeeded in performing such a study on some ferroelectrics[10,11] and rather complicated solid solutions $(La_{1-y}Eu_y)_{0.7}Pb_{0.3}MnO_3$ (y: 0.2; 0.6).[12,13]

Of particular interest is the study of different caloric effects in the same material, because its total caloric efficiency can be elevated by using simultaneously distinct external fields. As we know, only a few papers have been devoted to the simultaneous study of the barocaloric effect (BCE) and MCE in the same magnetic material; in particular, Ni-Mn-In alloys undergoing ferromagnetic and martensitic phase transitions in a narrow temperature range.[14,15]

Despite many solid solutions being composed on the grounds of $La_{0.7}Me_{0.3}MnO_3$ (Me: Pb, Ca, Sr) manganites, the information on their thermal properties is very poor. According to X-ray studies at room temperature,[16] $La_{0.7}Pb_{0.3}MnO_3$ (LPM) is characterised by rhombohedral symmetry (sp. gr. R-3c). Investigations of magnetic properties have shown a phase transition between paramagnetic and ferromagnetic phases at $T_0 = 353$ K. Earlier, both extensive and intensive MCE in $La_{1-x}Pb_xMnO_3$ (x: 0.1; 0.2; 0.3) solid solutions were evaluated for powder samples from measurements by indirect methods, as mentioned above.[8]

In this work, we have performed calorimetric, dilatometric, and differential thermal analysis (DTA) under pressure investigations on single crystal samples of LPM. The intensive magnetocaloric effect was measured directly using an adiabatic calorimeter. By analysing the entropy-temperature-pressure phase diagram, the intensive and extensive BCE in LPM were also determined and compared with MCE.

II. EXPERIMENTS

The method of spontaneous crystallisation from solution in a melt was used to grow LPM single crystals with a cubic

a)E-mail: akartashev@yandex.ru.

shape of the size of $3 \times 3 \times 3$ mm^3. To prevent Pb loss, a mixture of PbO/PbF_2 was taken as solvent.

The samples obtained were examined by X-ray diffraction and revealed, at room temperature, rhombohedral symmetry consistent with the data of Ref. 16. The crystallographic symmetry above paramagnetic-ferromagnetic phase transition was also found to be the same. No additional phases were observed in the samples.

The heat capacity study of LPM was carried out in the wide temperature range from 2 to 800 K by three calorimetric methods. Low temperature measurements between 2 and 300 K were performed using a PPMS calorimeter (Quantum Design, Inc., San Diego, CA) on a sample with a mass of 48.2 mg. Apiezon N grease was used to provide reliable thermal contact between the sample and the addenda. The heat capacity of the addenda was measured by individual experiment.

In the middle temperature range (150–370 K), calorimetric studies were carried out by means of a homemade adiabatic calorimeter with three screens described in Ref. 12. The LPM sample involving several single crystal pieces with total mass of 1.05 g was put into a heater, which consists of a polished aluminium foil container with constantan wire cemented to its inner surface. In order to provide a secure thermal contact between the sample and heater, we used vacuum grease. Using the heat capacity of the heater $C_h(T)$ determined in a separate experiment, information about the heat capacity of the sample $C_S(T)$ was obtained.

In the high temperature region from 370 up to 800 K, heat capacity was measured with a differential scanning calorimeter (Netzsch STA 449 C Jupiter). The mass of the sample was 18.7 mg. During the experiments on heating and cooling regimes at ± 5 K/min rate, argon gas-flow was maintained at a constant flow rate of 35 ml/min. The calorimeter was calibrated using standard materials In, Ag_2SO_4, $BaCO_3$, K_2CrO_4, and $KClO_4$. The error in heat capacity did not exceed 4% to 5%.

To study intensive MCE, we performed direct measurements of the temperature change at magnetic field variation using an adiabatic calorimeter. A platinum resistance thermometer attached to the adiabatic screen closest to the sample allowed us to monitor the temperature of the sample+heater system with high-precision. The long-term stability of this thermometer is rather high $\sim$0.002 K and the absolute accuracy of temperature measurements was ± 0.01 K. The temperature difference between the thermometer and the sample was monitored by a doubled copper-constantan thermocouple whose output was supplied to the automatic control circuit.[12]

The procedure of intensive MCE measurements was as follows. First, the sample was cooled (or heated) to some initial temperature in a rather wide temperature region, which included the phase transition point. The temperature drift of the sample was regulated to obtain an optimum rate of about $|dT/dt| \leq 3 \times 10^{-3}$ K/min. The switching on of magnetic field H led to abrupt increase of the sample+heater system temperature $\Delta T^{ON}{}_{EXP}$. Then, the temperature drift of the system was controlled and was found to be the same as observed before applying the field. The magnetic field shutdown was followed by a temperature decrease $\Delta T^{OFF}{}_{EXP}$ found to be equivalent to $\Delta T^{ON}{}_{EXP}$. Thus, there was a perfect reversibility of cycling $H = 0 - H \neq 0 - H = 0$. Figure 1 shows the results of ΔT_{EXP} measurements at 337 K and magnetic field varying between 0 and 5.4 kOe. Both values of $\Delta T^{OFF}{}_{EXP}$ and $\Delta T^{ON}{}_{EXP}$ are associated with the magnetocaloric response in the LPM sample and strongly elevated with the magnetic field increase. The uncertainty in the determination of ΔT_{EXP} was about $\pm 5\%$.

The temperature change of the sample+heater system ΔT_{EXP} recorded in the experiments with magnetic field is less than the value of real intensive MCE ($\Delta T^{MCE}{}_{AD}$). The reason for this is that the energy change of the sample associated with MCE under adiabatic variation of the magnetic field is spent to increase (or decrease) the temperature of both sample and heater. The values $C_h(T)$, $C_S(T)$, ΔT_{EXP}, and $\Delta T^{MCE}{}_{AD}$ are related by the equation,[12,13]

$$\Delta T_{AD}^{MCE} = \Delta T_{EXP}\left(1 + \frac{C_h}{C_S}\right), \tag{3}$$

which allows us to obtain information about the actual change in temperature of LPM in response to an adiabatically applied and removed external magnetic field.

The measurements of the thermal expansion were performed in the temperature range 100–900 K with a heating rate of 2–5 K/min using a NETZSCH model DIL-402C pushrod dilatometer. The ceramic sample was prepared from single crystals in the form of a cylinder (4 mm in diameter and 5.17 mm in length). The investigation was made under a helium atmosphere flowing at 40 ml/min. The results were calibrated using SiO_2 and Al_2O_3 as standard references, removing the influence of system thermal expansion.

The study of the hydrostatic pressure effect on the phase transition temperature in LPM was carried out on the same sample that had previously been used for the calorimetric measurements. DTA was used to detect the temperature associated with the heat capacity anomaly. A single crystal sample with a mass of 0.234 g was placed in a small copper container glued onto one of two junctions of a germanium-copper thermocouple. A quartz sample cemented to the other junction was used as a reference substance. The system, mounted in such a manner, was placed inside the piston-and-cylinder-type vessel associated with the multiplier. Pressure

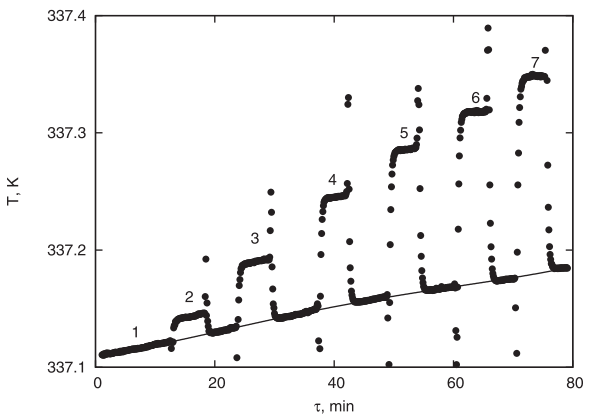

FIG. 1. Experimental temperature profile dependence of $La_{0.7}Pb_{0.3}MnO_3$ sample on the magnetic field change: 0.0 kOe (1), 1.1 kOe (2), 2.1 kOe (3), 3.2 kOe (4), 4.1 kOe (5), 4.8 kOe (6), 5.4 kOe (7).

up to 0.35 GPa was generated using silicon oil as the pressure-transmitting medium. Pressure and temperature were measured with a manganin gauge and copper-constantan thermocouple with accuracies of about $\sim 10^{-3}$ GPa, and ~0.3 K, respectively. The measurements were performed for both increasing and decreasing pressure cycles, to ensure the reliability of the results.

III. RESULTS AND DISCUSSION

In Figure 2(a), one can see the isobaric molar heat capacity $C_p(T)$ of LPM throughout the entire temperature region of measurements. The $C_p(T)$ peak was observed at $T_0 = 338.8 \pm 0.5$ K corresponding to the paramagnetic-ferromagnetic phase transition found earlier from the study of magnetic properties[16] at the higher temperature of $T_0 = 353$ K. The rather large difference between the values of phase transition temperatures determined from the present calorimetric data and those presented in Ref. 16 can be explained by the different approaches used to evaluate T_0. In Ref. 16, T_0 was determined as the temperature associated with the minimum value of the temperature derivative of magnetisation dM/dT. In accordance with thermodynamic theory,[17] a more correct way to determine T_0 is to analyse the derivative dM^2/dT. Indeed, the phase transition entropy ΔS is proportional to the square of the order parameter (magnetisation M in the case of LPM),[18]

$$\Delta S(T) = A_T M^2(T), \tag{4}$$

where A_T is one of the coefficients of thermodynamic potential,

$$\Delta\Phi = A_T \cdot (T - T_0) \cdot M^2 + B \cdot M^4 + C \cdot M^6 + \ldots - H \cdot M. \tag{5}$$

The dashed curve in Figure 2(a) represents the lattice heat capacity C_{lat} estimated by smoothed interpolation of the $C_p(T)$ data above and below the phase transition region by combination of the Debye and Einstein functions. Varying the temperature intervals included in the fitting procedure, we have found that the smallest average deviation of the experimental data from the smoothed curve does not exceed 0.5%. The anomalous part ΔC_p of the heat capacity was found in a rather wide temperature range between 367 and 180 K. The relation between the maximum value of excess heat capacity and C_{lat} is about 20%.

According to Eq. (4), excess entropy, as well as excess heat capacity, exists in the temperature region between the phase transition point and the temperature of M^2 saturation. This approach is valid for LPM as both values, M^2 and ΔC_p, are changed in the same temperature range ~ (T_0-160 K). The total excess entropy associated with ferromagnetic phase transition was evaluated as $\Delta S_0 = \int(\Delta Cp(T)/T)dT = 3.7 \pm 0.3$ J/mol·K and its temperature dependence is plotted in Figure 2(b).

The experimental data on $C_S(T)$, $C_h(T)$, as well as ΔT_{EXP} (T) were used to determine the values of the actual temperature change $\Delta T^{MCE}{}_{AD}$ of the LPM sample under magnetic field. In the case of LPM, anomalous heat capacity ΔC_p is about 15% of total heat capacity C_S. Usually, low field (up to 5 kOe in our case) leads to small changes of ΔC_p. Therefore, we can neglect the field dependence of C_S. The relation between $\Delta T^{MCE}{}_{AD}$ and ΔT_{EXP} described by Eq. (3) was kept at about 2.1 for all fields studied. Figure 3(a) shows the temperature variations of intensive MCE for a magnetic field ranging from 1.1 to 5.4 kOe. In all cases, a maximum value of $\Delta T^{MCE}{}_{AD}$ was found at about $T_{MAX} \approx 342$ K. It was pointed out above that the measurements of $\Delta T^{EXP}{}_{AD}$ (H) dependencies were followed by a rather small temperature drift. Indeed, the change of the sample temperature was less

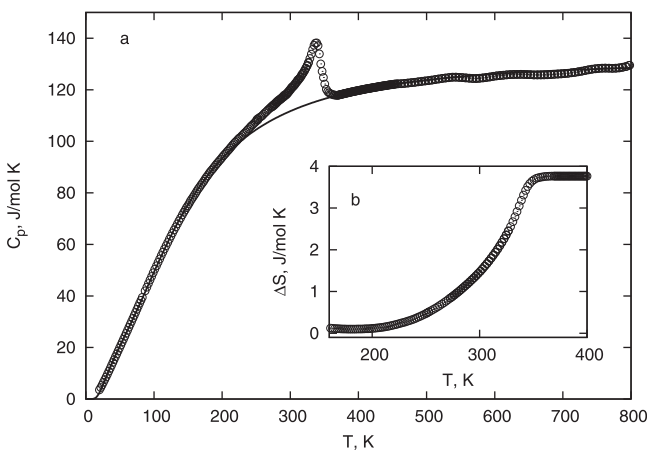

FIG. 2. Heat capacity of LPM as a function of temperature (a). Solid line is the lattice contribution. The behaviour of phase transition entropy (b).

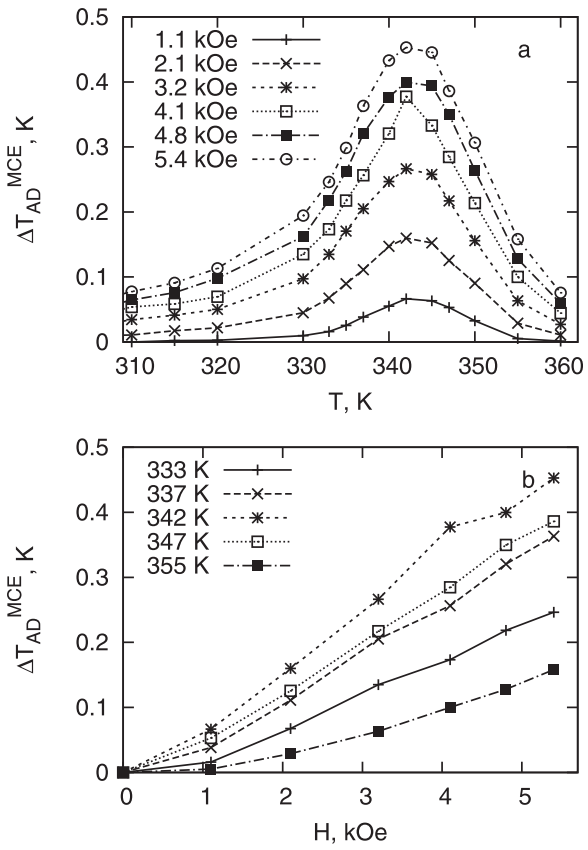

FIG. 3. Temperature dependence of the intensive MCE for constant fields (a). Values of $\Delta T^{MCE}{}_{AD}$ at the peak position plotted as a function of field for different temperatures (b).

than 0.07 K in a period of 80 min (Figure 1). Consequently, one can consider the dependencies of $\Delta T^{MCE}_{AD}(H)$ as isotherms (Figure 3(b)). It is seen that there is no evidence yet of the ΔT^{MCE}_{AD} value saturation with the field elevation, at least in the range of the magnetic field studied.

As mentioned above, materials showing simultaneously at least two pronounced caloric effects of different physical nature are of particular interest. The BCE is the most common effect characteristic of all thermodynamic systems including solid state systems. It refers to the adiabatic temperature change ΔT^{BCE}_{AD} or isothermal entropy change ΔS_{BCE} on the application or withdrawal of an external pressure,[1]

$$\Delta S_{BCE} = -\int_0^p \left(\frac{\partial V}{\partial T}\right)_{p,H} dp, \tag{6}$$

$$\Delta T^{BCE}_{AD} = -\frac{T}{C_{p,H}} \int_0^p \left(\frac{\partial V}{\partial T}\right)_{p,H} dp. \tag{7}$$

It is seen that both values depend on the thermal expansion of the material and can be conventional ($\Delta S_{BCE} < 0$, $\Delta T^{BCE}_{AD} > 0$) or inverse ($\Delta S_{BCE} > 0$, $\Delta T^{BCE}_{AD} < 0$) at $dp > 0$, in accordance with positive or negative volume change near the phase transition point. Therefore, the thermal expansion of material is one of the most important parameters characterising its barocaloric efficiency.

Figure 4(a) shows the temperature dependence of the coefficient of thermal volume expansion β. Its behaviour is characteristic for the second order transformation, as was also found earlier for the $C_p(T)$ dependence. Comparing the dependencies of $C_p(T)$ and $\beta(T)$ in the framework of the Pippard equation $C_p = (dp/dT)\cdot V\cdot T\cdot\beta + \text{const}$, one can obtain information about the susceptibility of a material to external pressure.[19] The linear dependence of C_p against β below T_0 was found in the temperature interval 310–325 K. The value of the initial baric coefficient characterising the shift of phase transition point under hydrostatic pressure was found to be $dT_0/dp = 0.75$ K/kbar. A calculation using the Ehrenfest equation gives a value $dT_0/dp = T_0(\Delta\beta/\Delta C_p) = 0.8$ K/kbar.

The pressure-temperature phase diagram of LPM was built from the results of DTA experiments under pressure, detecting the heat capacity anomaly associated with the phase transition (Figure 4(b)). The boundary between the paramagnetic and ferromagnetic phases can be described adequately with the baric coefficient $dT_0/dp = 1.75 \pm 0.5$ K/kbar. One can suppose that disagreements between the calculated and independently measured values of dT_0/dp can be ascribed to a different smearing degree of heat capacity and thermal dilatation anomalies in the vicinity of the phase transition point. In the DTA measurements, we did not observe any considerable changes of the phase transition enthalpy ΔH_0 with pressure increase. A small elevation of the phase transition temperature under pressure allowed us to think that the anomalous entropy $\Delta S_0 \approx \Delta H_0/T_0$ is almost constant in the range of pressure studied.

Considering the $C_p(T)$ and $T_0(p)$ dependencies, we have analysed BCE in LPM using the approach derived in Refs. 20 and 21 and successfully applied for the second order ferroelectric phase transitions.[10,11] Using this approach, we assume that low hydrostatic pressure effects, mainly on the magnetic subsystem, lead to the shift of the phase transition temperature in LPM. A substantial change in the lattice entropy S_{lat} is probably almost absent. Thus, the dependence $S_{lat}(T)$, determined at $p = 0$, can be used as the background entropy for the analysis of the pressure influence. The temperature dependences of the lattice entropy $S_{lat}(T)$ change in the temperature range investigated and the anomalous component $\Delta S(T)$ at ambient pressure were obtained by integration of the functions $C_{lat}(T)/T$ and $(C_p(T) - C_{lat}(T))/T$, respectively.

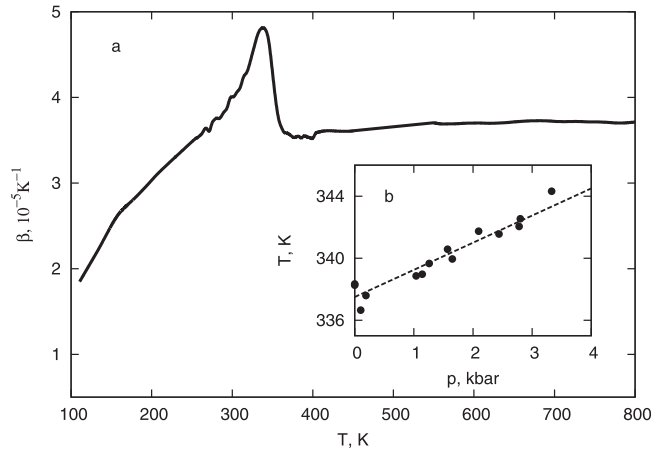

FIG. 4. Temperature dependence of the volume coefficient of thermal dilatation (a). Pressure dependence of phase transition temperature (b).

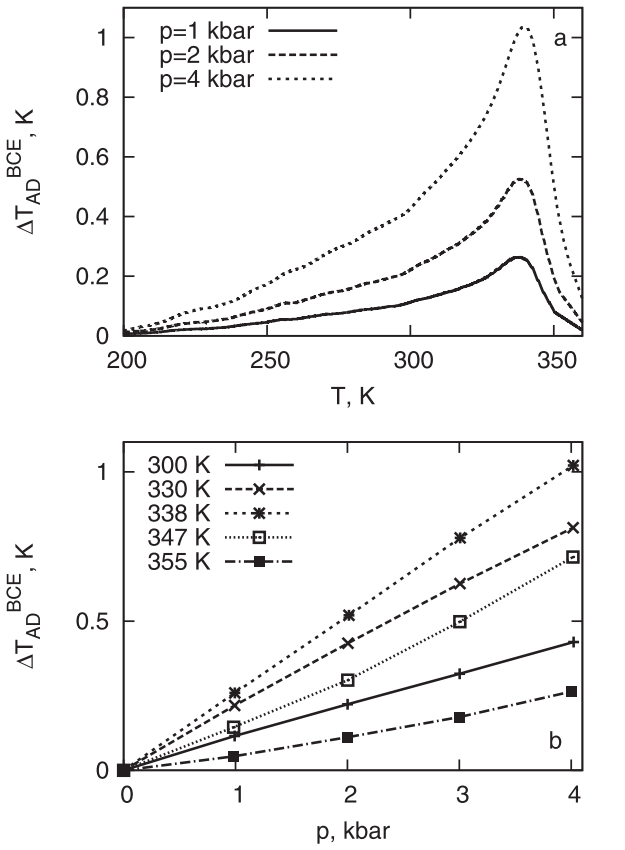

FIG. 5. Temperature dependence of the intensive BCE for constant pressure (a). Values of ΔT^{BCE}_{AD} at the peak position plotted as a function of pressure for different temperatures (b).

TABLE I. Some caloric parameters for $La_{0.7}Pb_{0.3}MnO_3$ and some related manganites. Phase transition temperature (T_0, K); specific maximum values of $(\Delta T^{MCE}{}_{AD})_{MAX}/\Delta H$ (K/kOe); $\Delta S_{MCE}{}^{MAX}/\Delta H$ (J/(kg·K·kOe)) and $(\Delta T^{BCE}{}_{AD})_{MAX}/\Delta p$ (K/kbar); $\Delta S_{BCE}{}^{MAX}/\Delta H$ (J/(kg·K·kbar)); normalised relative cooling power based on the adiabatic temperature change (RCP(T)/ΔH, K^2/kOe and RCP(T)/Δp, K^2/kbar) and on the isothermal entropy change (RCP(S)/ΔH, J/kg·kOe and RCP(S)/Δp, J/kg·kbar).

Composition	T_0	$\frac{(\Delta T_{AD}^{MCE})_{MAX}}{\Delta H}\times 10^2$	$\frac{(\Delta T_{AD}^{BCE})_{MAX}}{\Delta p}$	$\frac{\Delta S_{MCE}^{MAX}}{\Delta H}\times 10^2$	$\frac{\Delta S_{BCE}^{MAX}}{\Delta p}\times 10$	$\frac{RCP(T)}{\Delta H}$	$\frac{RCP(T)}{\Delta p}$	$\frac{RCP(S)}{\Delta H}$	$\frac{RCP(S)}{\Delta p}$
$La_{0.7}Pb_{0.3}MnO_3$ Single crystal	339	8.3 ± 0.4	0.25 ± 0.03	15 ± 0.9	4.3 ± 0.5	2.0 ± 0.2	10.5 ± 1.5	2.0 ± 0.2	14.7 ± 2.0
$La_{0.7}Pb_{0.3}MnO_3$ Ceramic[8]	349	5.0 ± 0.5[a]		6.4 ± 0.7[b]		2.0 ± 0.3			
$(La_{0.8}Eu_{0.2})_{0.7}$ $Pb_{0.3}MnO_3$ Single crystal[13]	310	3.8 ± 0.3[a]		5.0 ± 0.4		1.8 ± 0.2		2.4 ± 0.2	
$La_{0.7}Ca_{0.3}MnO_3$ Single crystal[2]	227	10.0 ± 1.2[b]		12.8 ± 1.4 [b]				4.7 ± 0.5	

[a]Data obtained by direct measurements.
[b]Data calculated from M(T, H) and C_p(T) dependences.

The entropy for $p > 0$ as a function of temperature and pressure, was determined by summation of the pressure independent regular lattice entropy $S_{lat}(T)$ and the anomalous contributions $\Delta S(T)$ at $p = 0$, shifted along the temperature scale according to the pressure dependence of the transition temperature $T_0(p)$ obtained experimentally $S(T,p) = S_{lat}(T) + \Delta S(T + (dT_0/dp)\cdot p)$.

The values of intensive and extensive BCE were determined at adiabatic $S(T,p = 0) = S(T + \Delta T^{BCE}{}_{AD}, p \neq 0)$ and isothermal $\Delta S_{BCE} = S(T,p \neq 0) - S(T,p = 0)$ conditions, respectively.

Temperature dependencies of $\Delta T^{BCE}{}_{AD}$ for LPM are presented for different values of pressure in Figure 5(a). It is necessary to point out that the temperature of the maximum values of BCE is very close to T_0. The reason for this is that extremums of the $C_p(T)$ and $(\partial V/\partial T)_p$ functions take place at almost the same temperatures.

The dependencies of $\Delta T^{BCE}{}_{AD}$ on pressure at $T = const$ were found to be linear (Figure 5(b)). Again, as in the case of $\Delta T^{MCE}{}_{AD}$ (Figure 3(b)), intensive BCE does not show saturation with external pressure increase, at least for those pressures studied.

In order to characterise materials as prominent solid state refrigerants, it is not enough to consider only the absolute values of entropy and temperature changes under variation of the conjugated external field. It was found in many cases that large measured or calculated values of ΔS_{CE} and ΔT_{AD} are not necessarily related to significant refrigerating efficiency of the material. More informative characteristics are those such as specific maximum values of $\Delta T^{MAX}{}_{AD}/\Delta Y$ and $\Delta S^{MAX}{}_{CE}/\Delta Y$, or normalised relative cooling power RCP(T)/ΔY and RCP(S)/ΔY (Y is generalised field—H or p). The latter parameters include the maximum magnitudes of intensive $\Delta T^{MAX}{}_{AD}$ or extensive $\Delta S^{MAX}{}_{CE}$ caloric effects, as well as the temperature range where these characteristics have optimum values,[1]

$$\Delta RCP(T)/\Delta Y = \Delta T^{MAX}{}_{AD} \cdot \delta T_{FWHM}/\Delta Y, \quad (8)$$

$$\Delta RCP(S)/\Delta Y = \Delta S^{MAX}{}_{CE} \cdot \delta T_{FWHM}/\Delta Y. \quad (9)$$

Here, δT_{FWHM} denotes the full width at the half maximum of $\Delta T_{AD}(T)$ or $\Delta S_{CE}(T)$ curves.

In Table I, the results of MCE and BCE studies on single crystal LPM are summarised and compared with those of other manganites. The value of extensive MCE was determined in accordance with Eqs. (1) and (2) as $\Delta S^{MAX}{}_{MCE} = -(C_p/T)(\Delta T^{MCE}{}_{AD})_{MAX}$. Of course, it is rather difficult to compare caloric efficiency of different physical nature. Nevertheless, one can see that in accordance with the parameters normalised to units of a conjugated external field, barocaloric efficiency of LPM is significantly preferable to that of magnetocaloric. This property is very useful for building the effective cycle of mixed (magnetic and baric) cooling using two kinds of external field. Recently, such a relation between baro- and magneto-caloric parameters was also observed for Ni-Mn-In alloy.[15] From our point of view, this phenomenon could be associated with a rather strong difference of the susceptibilities of phase transitions temperature to magnetic field and hydrostatic pressure. Indeed, the characteristic values for the compounds above are as follows: LPM $dT_0/dH = 0.1$ K/kOe, $dT_0/dp = 1.7$ K/kbar; Ni-Mn-In (Ref. 15) $dT_0/dH = -0.14$ K/kOe, $dT_0/dp = 1.8$ K/kbar. It is worth noting that the same situation concerning the relation between the baro- and electrocaloric effects was found also for ferroelectric NH_4HSO_4 undergoing phase transition of the second order $dT_0/dE = -0.5\,K\cdot(kV/cm)^{-1}$, $dT_0/dp = 14$ K/kbar.[10,11]

The values of $(\Delta T^{MCE}{}_{AD})^{MAX}/\Delta H$ and $\Delta S^{MAX}{}_{MCE}/\Delta H$, which are almost constant at magnetic fields above ~1 kOe (Figure 3(b)), are larger in single crystal LPM compared with those in both ceramic of the same composition[8] and single crystal solid solution $(La_{0.8}Eu_{0.2})_{0.7}Pb_{0.3}MnO_3$ previously studied by us.[13] There is only a small difference between the magnetocaloric parameters of LPM and $La_{0.7}Ca_{0.3}MnO_3$ single crystals[2] (Table I). However, taking into account the rather large value of RCP(S)/ΔH for the latter compound, it would be interesting, from our point of view, to study BCE in a calcium substituted manganite.

IV. CONCLUSIONS

We have performed calorimetric and dilatometric analyses and DTA under hydrostatic pressure investigations, as well as direct measurements of intensive MCE on $La_{0.7}Pb_{0.3}MnO_3$ single crystal. Information regarding phase transition entropy and the temperature-pressure phase diagram was obtained and allowed us to determine the temperature and pressure dependencies of BCE. Both magnetocaloric and barocaloric intensive effects increase linearly with an increase in magnetic field and pressure, respectively. Normalised to the units of external fields (H and p), barocaloric efficiency exceeds magnetocaloric

efficiency in LPM. Summarising the caloric properties studied, one can think that LPM can be used as an effective solid state refrigerant in a mixed cooling cycle built on MCE and BCE.

ACKNOWLEDGMENTS

This study was supported in parts by The Russian Foundation of Basic Research (Grant No. 12-02-31253-mol-a), Federal Special Program "Scientific and scientific-pedagogical staff of innovative Russia" (No. 8379), and Council on Grants from the President of the Russian Federation for Support of Leading Scientific Schools (Project No. NSh-4828.2012.2). Dr. Maxim S. Molokeev is acknowledged for the X-ray characterisation of the samples.

[1]A. M. Tishin and Y. I. Spichkin, *The Magnetocaloric Effect and its Applications* (Institute of Physics Publishing, Bristol and Philadelphia, 2003), p. 475.
[2]M. H. Phan, S. C. Yu, N. H. Hur, and Y. H. Jeong, J. Appl. Phys. **96**, 1154 (2004).
[3]Y. Sun, J. Kamarad, Z. Arnold, Z. Kou, and Zh. Cheng, Appl. Phys. Lett. **88**, 102505 (2006).
[4]M. Bejar, R. Dhahri, F. El. Halouani, and E. Dhahri, J. Alloys Compounds **414**, 31 (2006).
[5]R. Venkatesh, M. Pattabiraman, K. Rangarajan, S. Angappane, and J.-G. Park, J. Appl. Phys. **103**, 07B319 (2008).
[6]Y. Zhang, P. J. Lampen, T. L. Phan, S. Ch. Yu,H. Srikanth, and M. H. Phang, "Thermal properties, magneto- and barocaloric effects in La0.7Pb0.3MnO3 13" J. Appl. Phys. **111**, 063918 (2012).
[7]J. Gutiérrez, J. R. Fernández, J. M. Barandiarán, I. Orúe, and L. Righi, Sens. Actuators A-Phys. **142**, 549 (2008).
[8]S. G. Min, K. S. Kim, S. C. Yu, H. S. Suh, and S. W. Lee, IEEE Trans. Magn. **41**, 2760 (2005).
[9]A. R. Dinesen, S. Linderoth, and S. Mørup, J. Phys.: Condens. Matter **17**, 6257 (2005).
[10]I. N. Flerov and E. A. Mikhaleva, Phys. Solid State **50**, 478 (2008).
[11]E. A. Mikhaleva, I. N. Flerov, V. S. Bondarev, M. V. Gorev, A. D. Vasiliev, and T. N. Davydova, Phys. Solid State **53**, 510 (2011).
[12]A. V. Kartashev, I. N. Flerov, N. V. Volkov, and K. A. Sablina, Phys. Solid State **50**, 2115 (2008).
[13]A. V. Kartashev, I. N. Flerov, N. V. Volkov, and K. A. Sablina, J. Magn. Magn. Mater. **322**, 622 (2010).
[14]L. G. Medeiros, N. A. Oliveira, and A. Troper, J. Appl. Phys. **103**, 113909 (2008).
[15]L. Mañosa, D. González-Alons, A. Planes, E. Bonnot, M. Barrio, J. L. Tamarit, S. Aksoy, and M. Acet, Nature Mater. **9**, 478 (2010).
[16]N. Volkov, G. Petrakovskii, P. Böni, E. Clementyev, K. Patrin, K. Sablina, D. Velikanov, and A. Vasiliev, J. Magn. Magn. Mater. **309**, 1 (2007).
[17]L. D. Landau and E. M. Lifshiz, *Statisticheskaya fizika* (Nauka, Moscow, 1964), p. 567.
[18]K. S. Aleksandrov and I. N. Flerov, Sov. Phys. Solid State **21**, 195 (1979).
[19]N. G. Parsonage and L. K. K. Steveley, *Disorder in Crystals* (Clarendon, Oxford, 1978), p. 434.
[20]Th. Strässle, A. Furrer, A. Donni, and T. Komatsubara, J. Appl. Phys. **91**, 8543 (2002).
[21]M. V. Gorev, I. N. Flerov, E. V. Bogdanov, V. N. Voronov, and N. M. Laptash, Phys. Solid State **52**, 377 (2010).